Chapter 6

Directional Backlights for Time-multiplexed 3D Displays

As the advancement of image display from monochromic to color, each development is driven by pursuing ever more natural visions. Therefore, stereoscopic displays are seen to be the major advancement to provide human perception closer to reality. Conventional stereoscopic displays can only show the depth effect, for example, when viewers wear special polarized glasses.[1] However, unnatural feelings reduce human desire to perceive natural visions. To do without special polarized glasses, autostereoscopic displays are therefore developed. In this chapter, autostereoscopic displays using time-multiplexed approach will be introduced. A directional backlight with a fast switching liquid crystal panel sequentially projects images to left and right eyes respectively, thus, achieving the 3D image perception.

6.1 Introduction

Recently, autostereoscopic displays, which do not require a user to wear special polarized glasses, are rapidly developed. Autostereoscopic displays can be generally classified into the “holographic type”, the “volumetric type” and the “stereo pairs’ type”. Nevertheless, the holographic approach is usually constrained in monochromic applications.[2] Besides, the volumetric type, which uses a laser beam to project the sketch of an object on a fast spinning plane, requires a bulky volume against the trend of thinness and light weight of display technologies.[3] The stereo pairs’ type, which can be further classified into the “spatial-multiplexed type” and the

“time-multiplexed type”, therefore becomes the most popular approach because of the compatibility with current LCD technologies. For the spatial-multiplexed type, odd and even pixels of panel control projected images to left and right eyes, respectively. Using the lenticular plate[4] and the parallax barrier[5] are the most general approaches to obtain two emitting cones of light to respective eyes. Contrarily, for the time-multiplexed type, images are projected to left and right eyes sequentially. In the following sections, we will concentrate on the “spatial-multiplexed type” and the “time-multiplexed type” and discuss in details.

Spatial-multiplexed Type

6.1.1. Lenticular Plate

Using a lenticular plate is one feasible approach to achieve 3D image perception. Because a lenticular plate can be easily fabricated by micro-machining and injection molding, it is advantageous in low price. Additionally, a lendicular plate is very light and thin for small sized applications. However, as the size of screen increasing, a lenticular plate becomes more difficult in fabrication. The heavy weight and the high price usually constrain its application. In 1990, Sanyo and Toppan first demonstrated 40” 3D display that uses the plasma display with a lenticular plate. Nevertheless, as the rapid grow of LCDs, more attentions are concentrated on LCD applications. LCD pixels shown in Fig. 6-1 are divided into odd pixel and even pixel pairs, which control the images to the left and right eyes, respectively. Then, by using a lenticular plate, two emitting cones of light are projected to respective eyes.

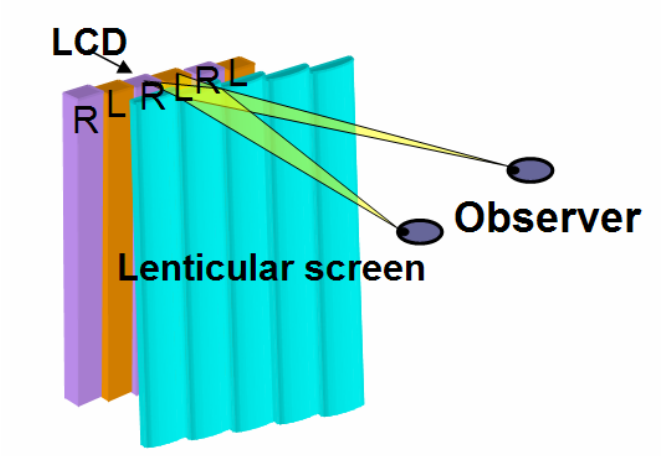

Fig. 6-1. Principle of lenticular plate to project two images to the respective eyes.

Recently, Philips proposed a novel 3D display that places a lenticular plate over the LCD at a slightly slanted orientation shown in Fig. 6-2. This technology can avoid moiré patterns caused by the superposed periodic structures, such as lenticular plates and LCD pixels. Additionally, the reduction of resolution can be averaged to both horizontal and vertical directions.

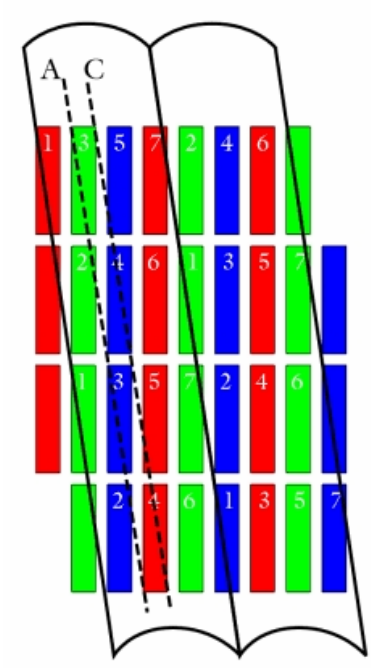

Fig. 6-2. Design of Philips' slanted lenticular plate.[15]

6.1.2 Integral Imaging

Recently, the integral imaging (InIm) has attracted much attention as an appealing 3D display technology because InIm provides continuous viewpoints within a specific viewing angle. In addition, full parallax along both horizontal and vertical directions can be obtained by the InIm approach. As shown in Fig. 6-3, 3D images are formed by integrating the rays coming from 2D elemental images using a lenslet or a pinhole array. The 2D elemental images can be generated by computer graphics on the CCD or LCD devices. InIm can provide observers with true 3D images with full parallax and continuous viewing points, as in holography. However, some drawbacks, such as the viewing angle, depth of focus and resolution of 3D images are limited in the InIm approach because lenslet arrays are used.[16][17] Constraints in f-number of lenslet arrays limit the mentioned optical performances of InIm.

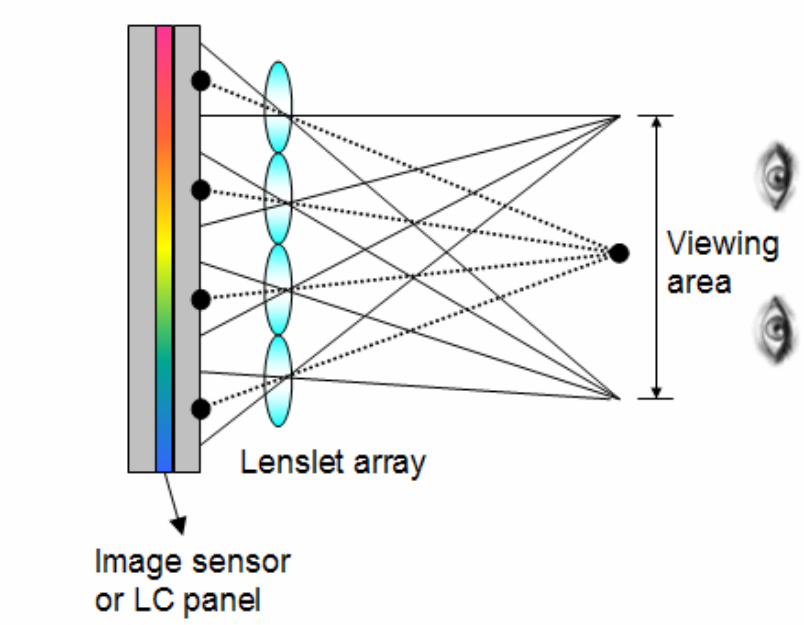

Fig. 6-3. Schematics of 3D integral imaging.

6.1.3 Parallax Barrier

The parallax barrier, which consists of interlaced black and transparent stripes, is placed at a fixed distance from the LC panel as shown in Fig. 6-4. Because the

period of the parallax barrier plate is approaching to that of the LC pixels, left and right eyes can observe the pixels of odd and even stripes, respectively. The position of the parallax barrier can be located between the LC panel and the viewer, as shown in Fig. 6-4(a). Besides, the parallax barrier can be also placed between the backlight and the LC panel as shown in Fig. 6-4(b).

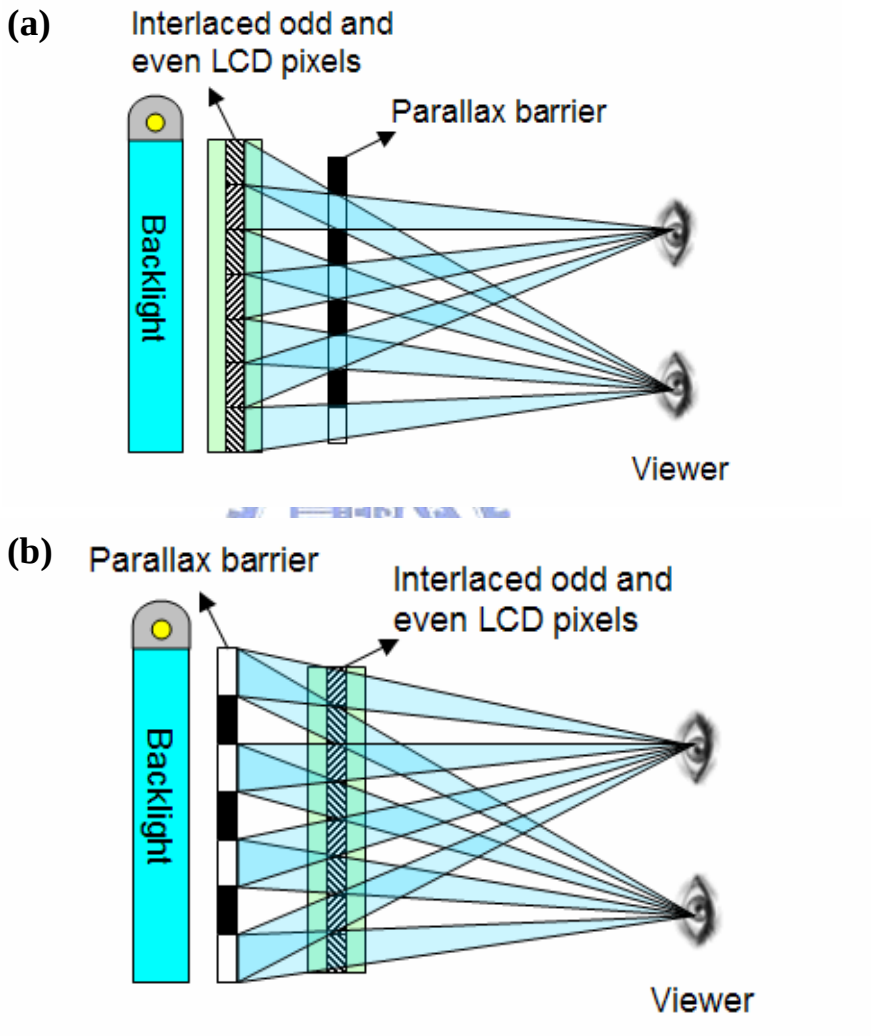

Fig. 6-4. Schematics of the parallax barrier placed between (a) the LC panel and the viewer (b) the LC panel and the backlight.

Except distinguished by the position of the parallax barrier, barrier systems can be classified into several configurations according to the operational principles. For first configuration, parallax barrier is fabricated by precisely printed black stripes.

However, printed parallax barrier is a passive device that can not automatically control the 2D/3D image conversion. In order to achieve 2D/3D conversion, a polymer dispersed liquid crystal (PDLC) panel is inserted between the parallax barrier and the LC panel as shown in Fig. 6-5.[6] Droplets of nematic liquid crystals embedded in a polymer binder are namely PDLC.

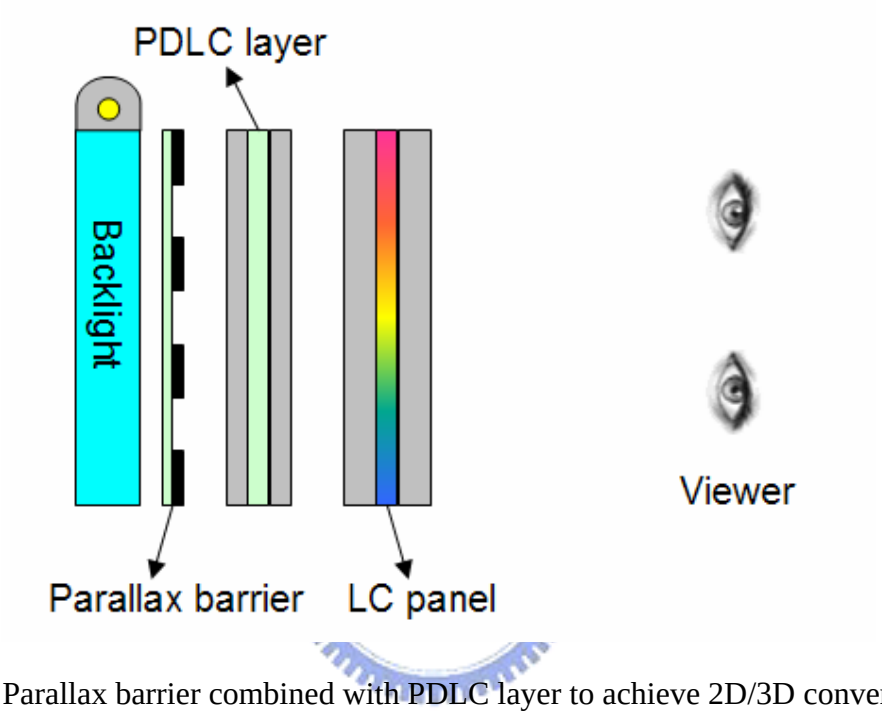

Fig. 6-5. Parallax barrier combined with PDLC layer to achieve 2D/3D conversion.

The droplets usually contain the LC molecules in a bipolar configuration. In the off-state of PDLC, the droplets are oriented at random as shown in Fig. 6-6(a). As a result, the index n_f of molecules differs from the index n_p of the polymer binder. The incident unpolarized light is hence refracted and reflected, resulting in scattering of the light in a wide angle towards the viewer. In the on-state shown in Fig. 6-6(b), the directors of the LC molecules orient themselves parallel to the electric field, exposing the refractive index n_o to the light. The polymer is to exhibit an index $n_p \cong n_o$. In the index matched state, light can consequently pass the transparent layer. As a consequence, we can utilize the characteristics of PDLC layer. For the operation of

the 3D mode, we applied a voltage on the PDLC layer. After passing through the parallax barrier plate, light seems to be passing through a transparent layer. Therefore, this configuration works as the schematics shown in Fig. 6-4(b). Contrarily, in the 2D mode, we do not apply any voltage. Light is hence scattered by the PDLC layer, thus, broadening the angles of light and destroying its directionality. Our eyes will observe the images of odd and pixels simultaneously. Therefore, this configuration is operating in 2D mode.

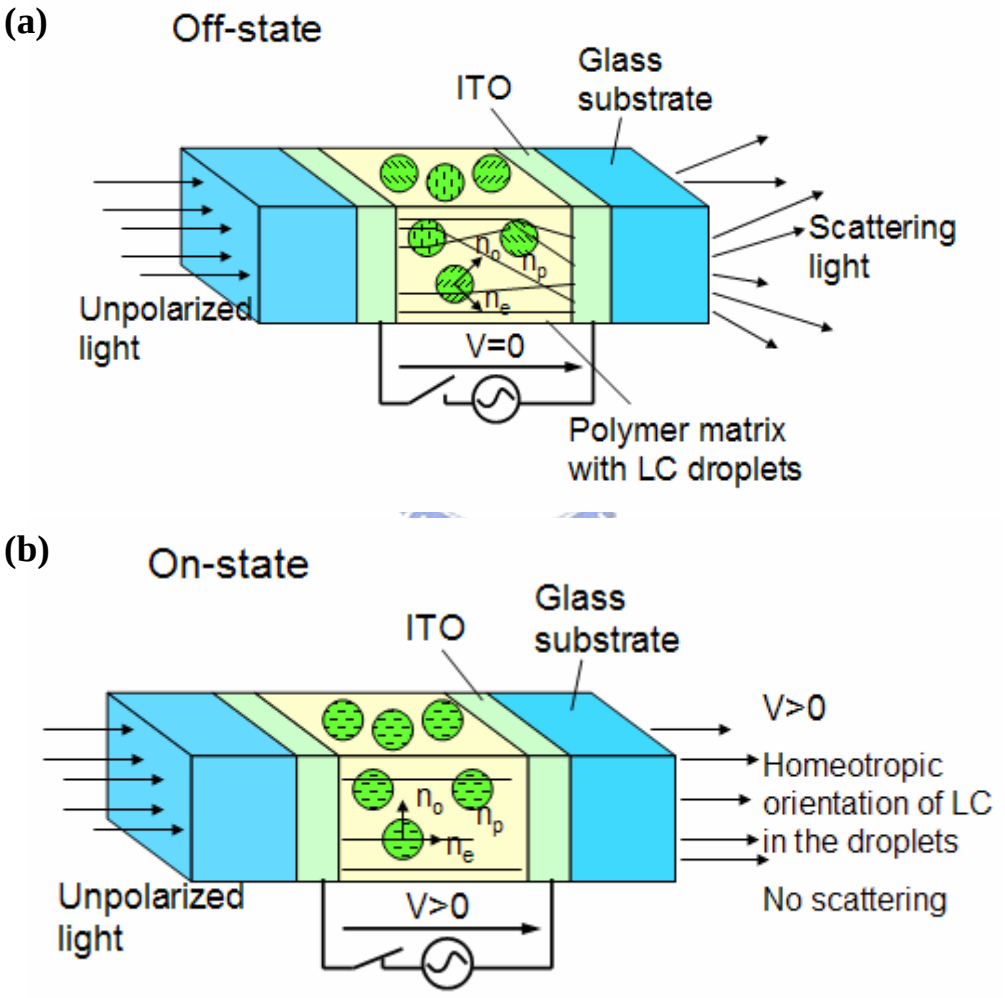

Fig. 6-6. Operation of the PDLC layer (a) in the off-state and (b) in the on-state.

For the second configuration, the parallax barrier is made by an additional LC panel as shown in Fig. 6-7.[7] In the 3D mode, we can switch on and off between the

interlaced pixels to treat the additional LC panel as the parallax barrier plate. In the 2D mode, we switch on all the pixels and the additional LC panel works as a transparent plate. Compared with the previous configuration, light is not scattered by the PDLC layer during the 2D/3D conversion. Therefore, this configuration using the additional LC panel provides higher transmission of light and brighter image. Besides, it does not smear the image on the panel.

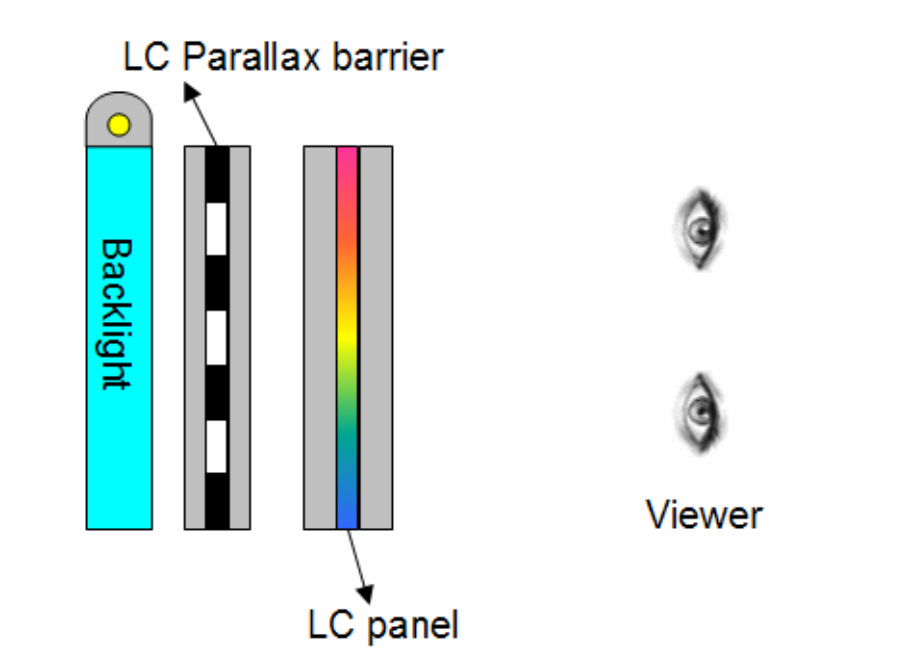

Fig. 6-7. Parallax barrier made by an additional LC plate to achieve 2D/3D conversion.

For the third configuration, the parallax barrier plate is made by the polarization modifying layer, which is consist of interlaced 0 and λ/2 phase retardation films. As schematically shown in Fig. 6-8, the polarization modifying layer, which is attached on the rear polarizer, is placed between the backlight and the LC panel. Therefore, for linearly polarized light, the polarization modifying layer behaves as interlaced black and transparent stripes. Contrarily, for unpolarized light, the polarization modifying layer does not appear the effects of the parallax barrier

plate.[8] Therefore, in order to achieve 2D/3D conversion, a rolled polarizer is placed between the lamp and the lightguide. For 2D mode, the polarizer is removed. In contrast, for 3D mode, the polarizer is inserted.

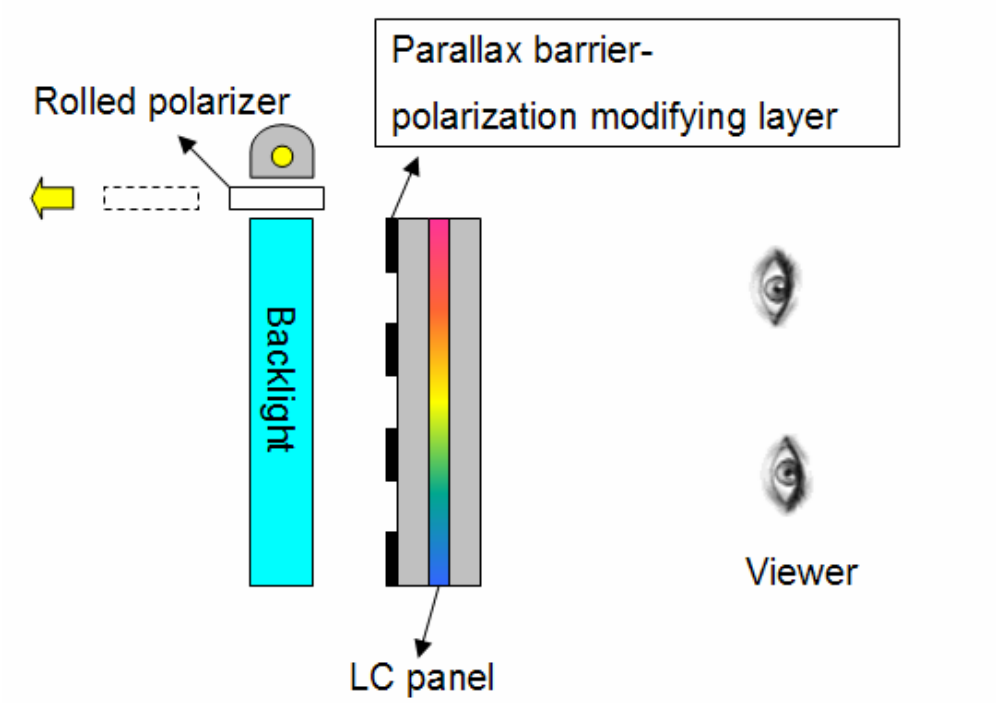

Fig. 6-8. Parallax barrier made by the polarization modifying layer to achieve 2D/3D conversion.

However, for previously mentioned spatial-multiplexed approaches, LCD pixels need to be divided into odd and even pixel pairs, thus, resulting in resolution of one half or less. In addition, the parallax barrier plate usually blocks parts of light from the backlight module and hence degrades the light utilization efficiency. Furthermore, critical alignment between the parallax barrier plate and LCD pixels is a serious concern. In order to solve the concerned issues, time-multiplexed approaches are developed.

Time-multiplexed Type

For spatial-multiplexed type, all view fields are presented simultaneously no

matter how many view fields there are. For time-multiplexed type, the view fields are sequentially presented. The most famous time-multiplexed 3D display shown in Fig. 6-9 was proposed by A. Travis in Cambridge University.[9], yet, constrained its applications by the huge volume of the display system.

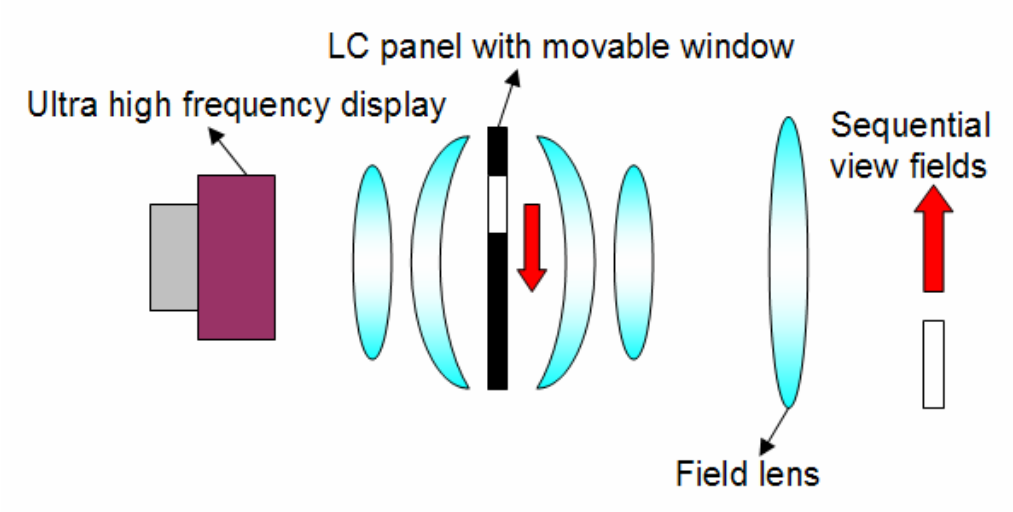

Fig. 6-9. Schematics of time-multiplexed 3D displays.

In the year of 2000, NHK demonstrated a 3D plasma display with shutter glasses. Interlaced images are observed by respective left and right eyes by fast switching on the shutter glasses. It is advantageous in wide viewing angle and no limitation in number of viewers. However, the viewer needs to wear shutter glasses. We proposed a novel time-multiplexed display with compact size without the need of wearing shutter glasses in the next section.

6.2 Theory

A compact time-multiplexed 3D display was proposed by using a switching, directional backlight combined with a fast switching LCD. Two restricted viewing cones were sequentially emitted from switching backlight. Two sates of image (Image observed in various viewing angles) were therefore obtained in our left eyes and right

eyes, respectively. The fast switching LC panel was then utilized with the directionally switching backlight to achieve binocular disparity. As shown in Fig. 6-10, the image was sent to the left eye in first state. Then, the image was sent to the right eye in another state.

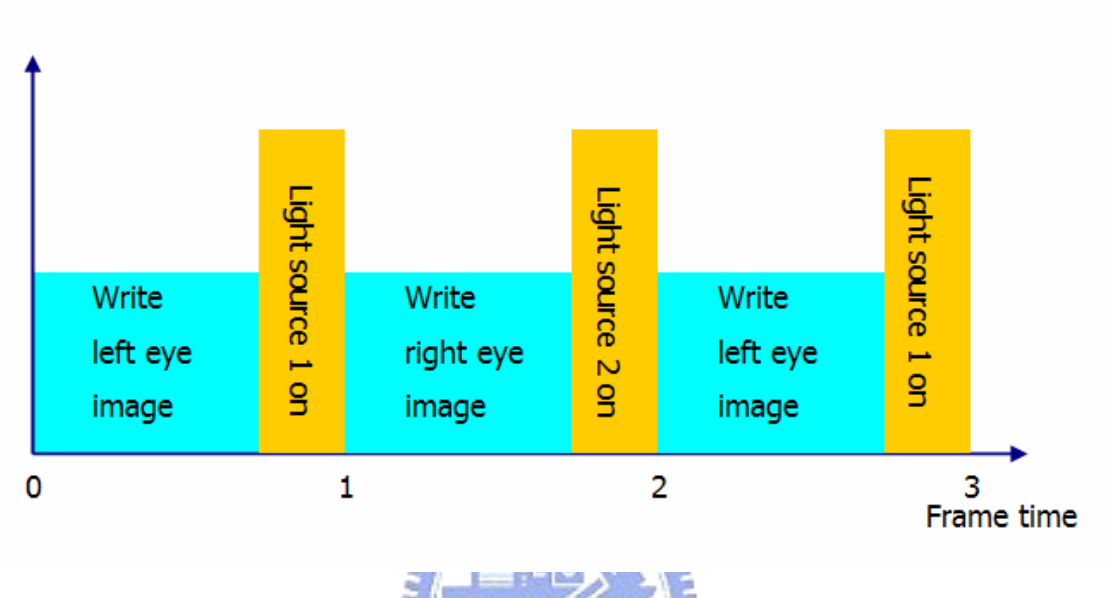

Fig. 6-10. Operating Principle of the proposed time-multiplexed 3D display.

A directional backlight consists of a micro-grooved lightguide in combination with a focusing foil as schematically shown in Fig. 6-11. When the light source was switched on, a large inclined angle of viewing cone was emitted from a micro-grooved lightguide. A total internal reflection occurred at the interface of the focusing foil, which was followed by a refraction of the large inclined light. A focusing foil therefore redirected the light to the viewer's eyes. According to the geometric calculations [Fig. 6-11(a)], the relationship between θ, θ′, θ″ and θ''' can be obtained from Equations (6-1), (6-2) and (6-3). Using Equation (6-3) by replacing θ′ and θ″ in Equations (6-1) and (6-2), the emitted angle of directional backlight was derived as Equation (6-4).

$$n \times \sin\theta' = \sin[\theta - (\alpha - \beta_1)] \qquad (6\text{-}1)$$

$$\theta'' = \beta_1 + \beta_2 - \theta' \quad (6\text{-}2)$$

$$\beta_2 - \theta''' = 90^\circ - \theta'' \quad (6\text{-}3)$$

$$\theta''' = 2 \times \beta_2 + \beta_1 - 90^\circ - \sin^{-1}\left(\frac{\sin(\theta - \alpha + \beta_1)}{n}\right) \quad (6\text{-}4),$$

where θ is the emitted angle from the grooved lightguide, θ′ is the refracted angle at the left side interface of grooves, θ″ is the incident angle at the right side interface of grooves, θ''' is the emitted angle of the directional backlight, β_1 and β_2 depict the composed vertex angles of asymmetric focusing foil, α is the half vertex angle of grooved lightguide, and n is the refractive index of the focusing foil. From Equations (6-1) and (6-4), it is clear that the emitted angle from the grooved lightguide increases when the vertex angle (2α) of the grooved lightguide becomes larger. Hence, the emitted angle θ''' from the backlight becomes larger as well. In addition, θ''' increases when the vertex angle ($\beta_1 + \beta_2$) of the grooved lightguide becomes larger. Consequently, the emitted angle of directional backlight can be determined by the vertex angles of asymmetric focusing foil and grooved lightguide. The desired angular distributions to the left and right eyes were therefore achieved by modifying a grooved lightguide with a focusing foil.

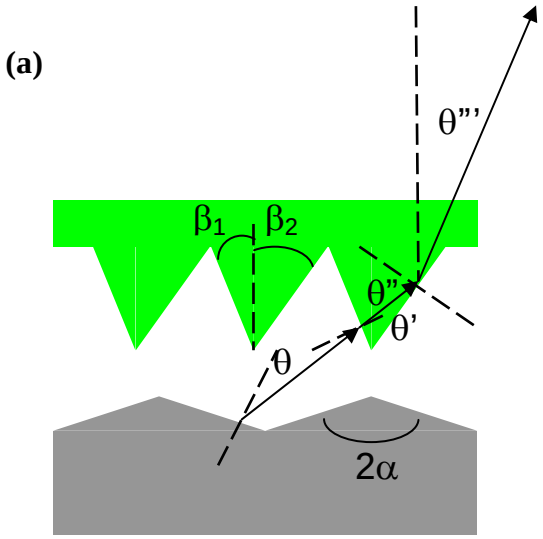

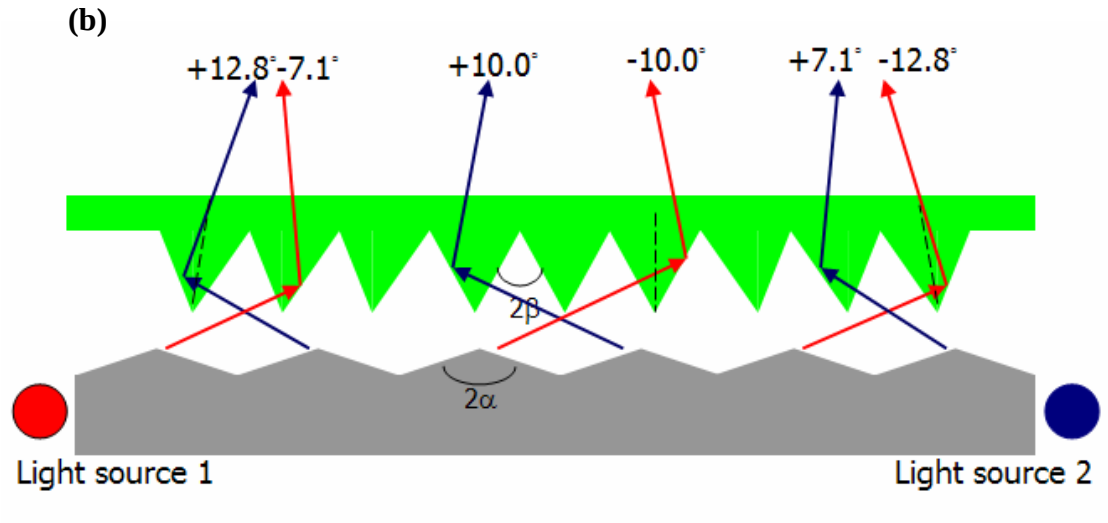

Fig. 6-11. (a) Schematics of a directional backlight. (b) A large inclined angle of viewing cone was emitted from a micro-grooved lightguide. An asymmetric focusing foil was then utilized to redirect light to the eyes.

In the thesis, we will focus on mobile applications. Following benefits were concerned to concentrate on a specific market.

(i) Single viewer was more or less predicted his relative position to display. Head tracking system becomes unnecessary.

(ii) Mobile applications were growing rapidly. High potential in market was expected to improve user interface by 3D image.

A schematic of observer's relative position and viewing angle to the display was illustrated in Fig. 6-12. A backlight of size of 35 mm (l) × 28 mm (w) was placed at a viewing distance of 185 mm. The distance between the left and the right eyes was estimated around 65 mm. Observer's left and right eyes were located around -10° and 10° to the normal viewing direction, respectively. Two sets of light sources were switched on sequentially to emit light to the left and the right eyes, respectively.

For focusing the light by different indicated viewing angles in their respective regions, asymmetrical micro grooves were used to redirect light propagation. A slant

of grooves becomes steeper while the other slant is gentler. For example, assuming the vertex angle of grooved lightguide is 165°, the emitted angle θ of 67.5° from the grooved lightguide was obtained by ray tracing. The refractive index of the focusing foil is set to be 1.49. For the middle region of the backlight, $\beta_1 = \beta_2$ and $\theta''' = -10^\circ$ were assumed. As a result, $\beta_1 = \beta_2 = 30^\circ$ can be obtained according to Equation (6-4). In consideration of easiness of fabrication, 60° of top angles of asymmetrical grooves remain constant. Nevertheless, the emitted angle θ''' of the directional backlight will be shifted due to the rotation of the groove's slant by a factor of 2. Therefore, in order to satisfy the defined angles -7.1° and -12.8° for the left-handed and the right-handed regions, (β_1, β_2) are designed to be (31.5°,28.5°) and (28.5°,31.5°) due to the shift of the emitted angle θ''' of approximately 3°. In other words, from the left-handed to the right-handed regions, the symmetric axis of grooves rotates from 1.5° to -1.5° in gradient. Consequently, light is redirected to the right eye by the defined angles. Similarly, light is focused to the left eye when the other light source is switched on.

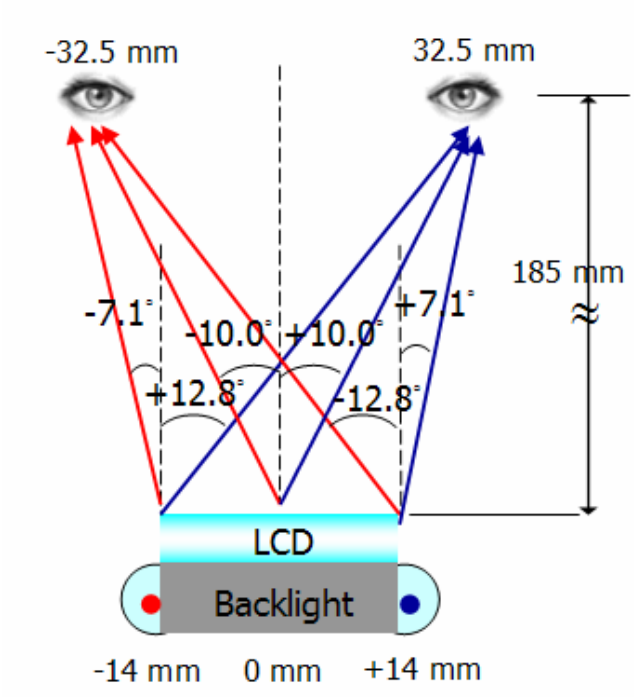

Fig. 6-12. Schematics of observer's relative position and viewing angle to the display.

6.3 Simulation

The model of 3D mobile display was built, shown in Fig. 6-13, by the optical design and analysis program “ASAP”, developed by Bro.

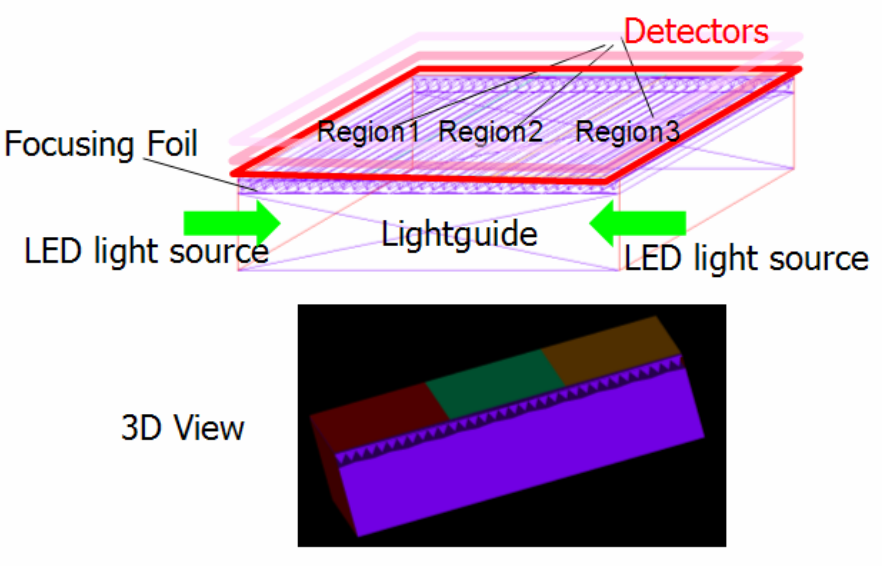

Fig. 6-13. Schematics of a micro-grooved lightguide and an asymmetrical focusing foil were built by ASAP.

A micro-grooved lightguide and an asymmetrical focusing foil were built. Light source 1 and 2 were both lambertian light sources. Array of detectors were utilized to observe the angular distributions in various regions.

The angular distributions of only micro-grooved lightguides were simulated by tuning the vertex angles of grooves as shown in Fig. 6-14. Two observed viewing cones were inclined large angles with respect to the viewer when both light sources were switched on. As the vertex angle of grooves was increasing, the inclined angle of viewing cone was becoming larger. From the simulated results, we can find that viewing cones were distributed in ±60° when the vertex angle of grooves equaled to 140°. Viewing cones were shifted to ±70° when the vertex angle of grooves equaled to 170°.

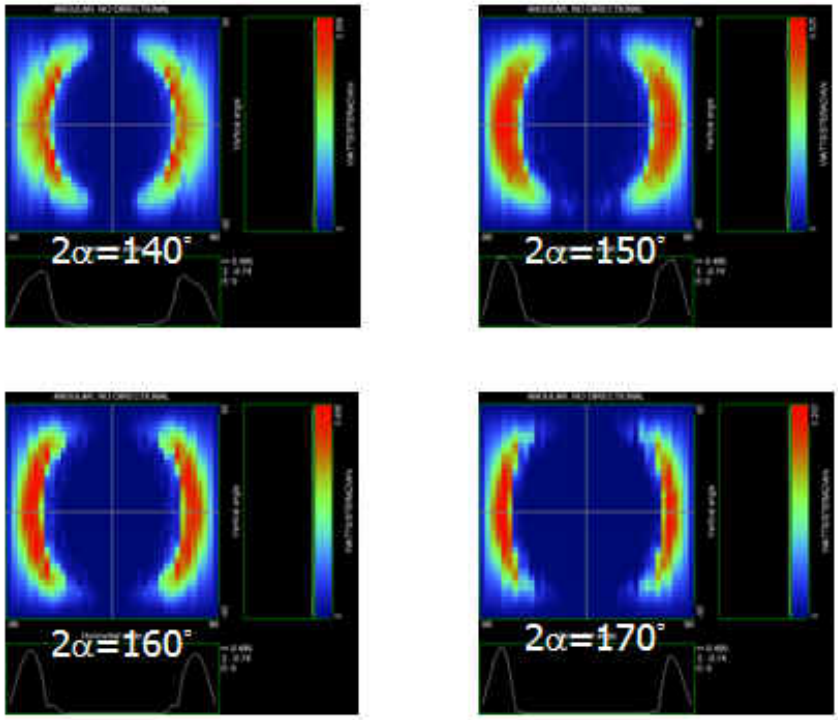

Fig. 6-14. Angular distributions of micro-grooved lightguide only by tuning the vertex angle of groove.

From the simulated results, the emitted angular cones of the grooved lightguide are distributed between 60° and 70° with respect to the normal direction. In order to redirect the emitted cones toward the viewer's eyes, which are located at approximately 10° with respect to the normal direction, the focusing foil is essential. From the above geometric calculations, the vertex angle of the focusing foil is estimated to be 60°. We summarized all the simulated parameters in the model as following.

Parameters of lightguide:

Size of lightguide= 35 mm× 28 mm× 1 mm
Vertex angle of lightguide= 165°
Groove pitch of lightguide= 100 μm
Vertex angle of focusing foil= 60°
Groove pitch of focusing foil= 57 μm

Parameters of focusing foils:

Region 1 (β_1, β_2)=31.5°, 28.5°

Region 2 (β_1, β_2)=30°, 30°

Region 3 (β_1, β_2)=28.5°, 31.5°

We illustrated the simulated angular distribution of the grooved lightguide in combination with the asymmetric focusing foil when light source 1 is switched on as shown in Fig. 6-15. Figs. 6-15(a), (b) and (c) represented the angular profiles for region 1, region 2 and region 3, respectively. The maximum brightness intensity of the angular profiles occurs at -7°, -10° and -13° for region 1, region 2 and region 3, respectively, which are satisfied the desired angular distributions, which are indicated in Fig. 6-12.

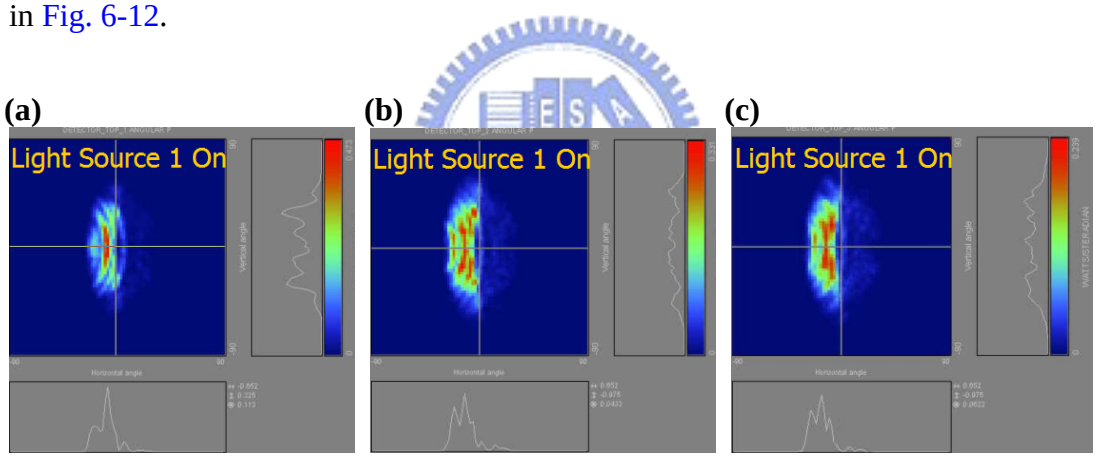

Fig. 6-15. Angular distributions of the grooved lightguide in combination with the asymmetric focusing foil for region (a) 1, (b) 2, and (c) 3.

6.4 Fabrication

We adopted the micro-machining process to fabricate the micro grooves of lightguide and the focusing foils. Fabrication procedures were followed by the steps shown in Fig. 6-16.

(i) Diamond knife was moved vertically to fabricate single groove on PMMA

(ii) Diamond knife was horizontally moved by the pitch of groove, then moved

vertically to fabricate grooves on PMMA

(iii) Edge of PMMA was flattened

(iv) Diamond knife was slightly rotated to fabricate asymmetric grooves of the focusing foil. In left side region, knife was rotated in positive direction. In center region, knife was remained in normal direction. In right side region, knife was rotated in negative direction.

(v) In order to stabilize the focusing foils on the display, thin focusing foils were attached on polarizers in combination with an LCD panel.

(vi) PMMA lightguide was assembled to focusing foils.

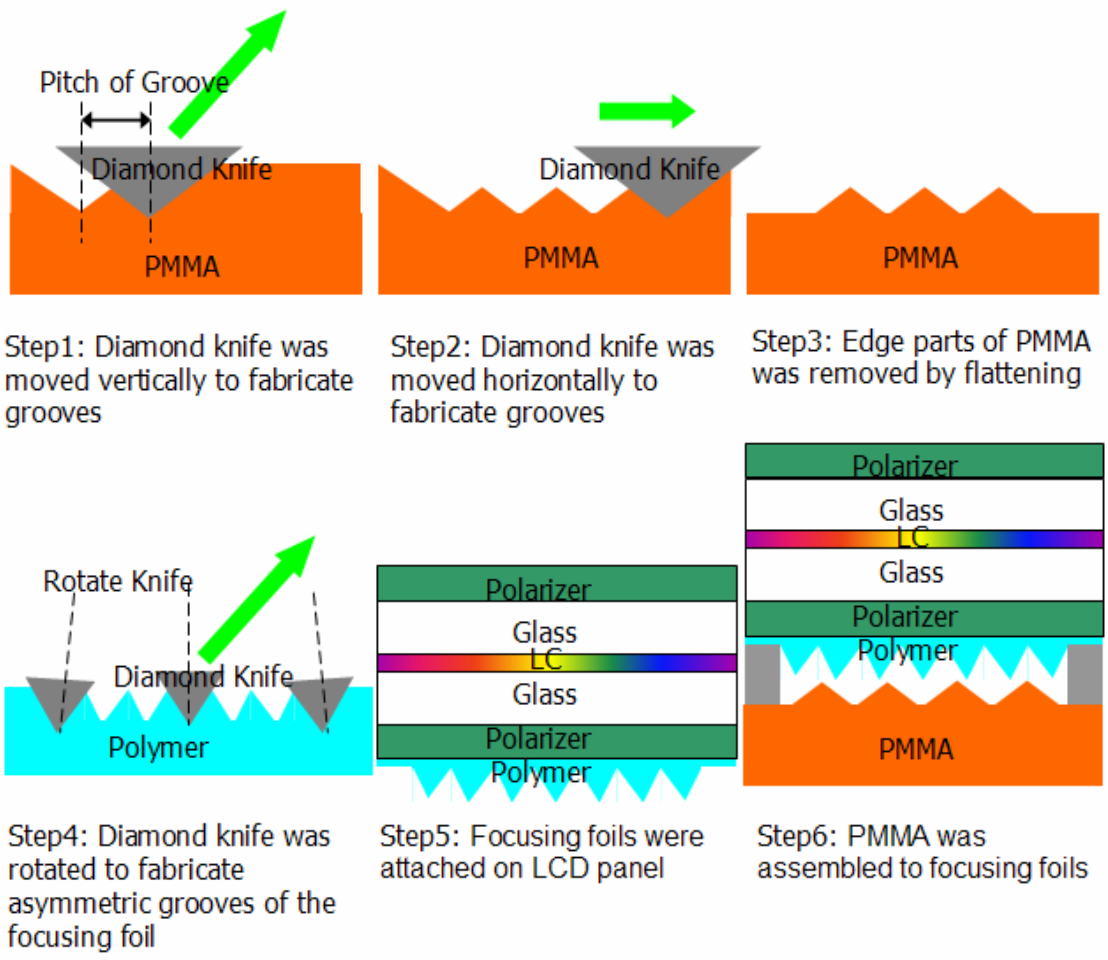

Fig. 6-16. Fabrication procedures of the grooved lightguide in combination with the focusing foil.

6.5 Measurement

The measurement setup was schematically illustrated in Fig. 6-17. Using white light LEDs with light bars as side-illuminated light sources, angular distributions of emitting light from the backlight module were measured by EZcontrast 160. Using backlight brightness intensity of 2100 cd/m^2, Figs. 6-18(a) and (b) depict the measured angular distributions of directional backlight with LC panel by sequentially switching the left and right side LEDs, plotted as a function of azimuth angle and the inclination angle, θ', respectively. Azimuthal angle defined the rotation of the detecting plane of inclination ranges from 0˚ to 360˚. In contrast, the inclination angle defined the radial position of the detecting plane, ranges from 0˚ to 80˚. According to the measurement of Fig. 6-18(a), most of light was distributed between the inclination angle of -30˚ and 0˚ when left side LEDs switched on.

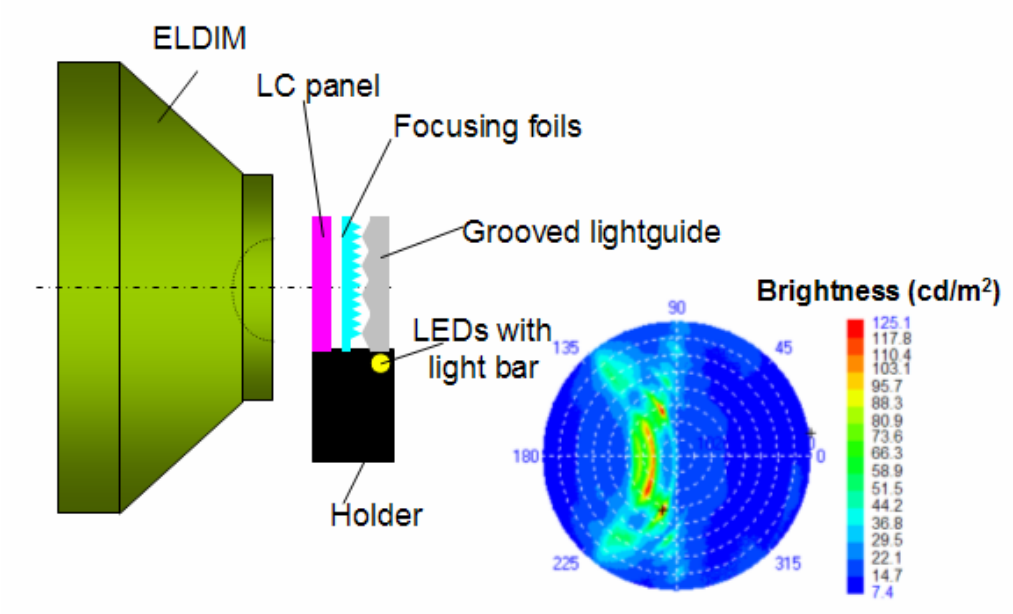

Fig. 6-17. Schematics of measurement setup.

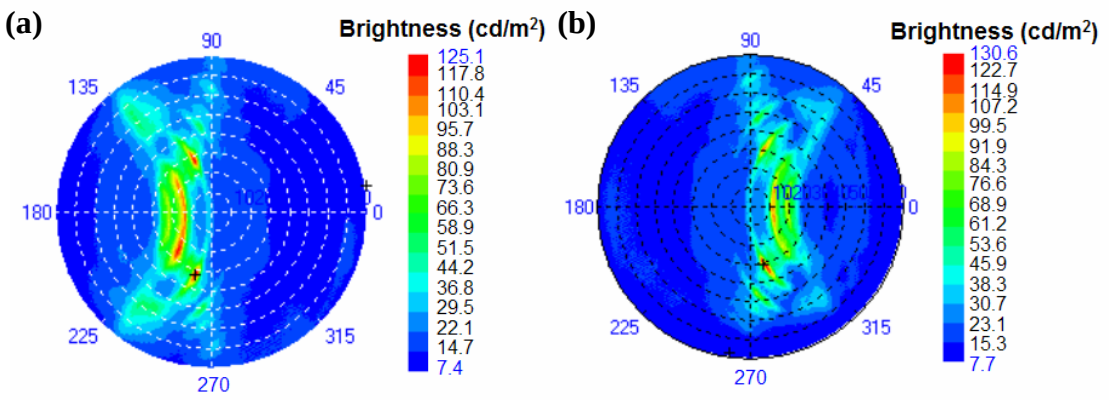

Fig. 6-18. Using backlight brightness intensity of 2100cd/m^2, angular distributions of the backlight module with LC panel when (a) left and (b) right side LEDs switched on.

For ϕ'=90˚ cross-section, the curves depict the dependence of luminance on different viewing angle of simulation and measurement, respectively, as shown in Fig. 6-19.

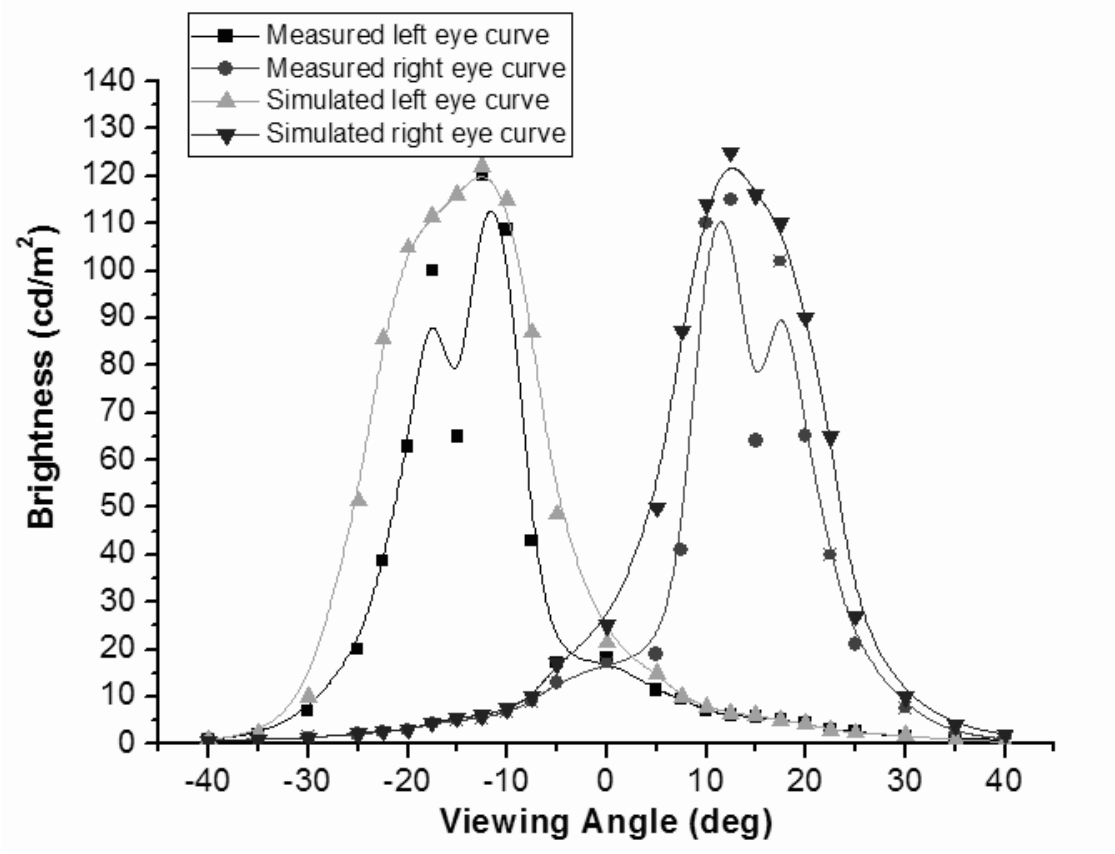

Fig. 6-19. For ϕ'=90˚ cross-section, the simulated and measured brightness intensity dependences on viewing angles.

6.6 Concerned Issues

From the measurement, we know that the measured curve is closely agreed with the simulated curve. However, some issues, such as moiré patterns, crosstalk and response time of LC, need to be further considered.

Moire patterns

The grooves of lightguide, the grooves of the focusing foil, and LCD pixel are periodic structures. After overlapping these periodic structures, it arouses moiré patterns. In order to suppress the moiré patterns, the pitch ratio of the grooved lightguide to the focusing foil is designed to be less than 3, so that the periods of moiré patterns is too small to be distinguish for our eyes.

Crosstalk

Ideally, when left side LEDs switched on, only left eye can observe the image. Practically, after propagating in the lightguide, some rays are reflected by the end surface of the lightguide, thus, causing crosstalk to the other eye.[10] Conventionally, crosstalk is of less than 10%, which is the minimum criterion to produce stereoscopic image perception for our brain.[11] As shown in Fig. 6-19, the measured luminous intensity is 109 cd/m^2 at viewing angle of -10˚ (left eye) while 7 cd/m^2 at viewing angle of 10˚ (right eye), thus, resulted in a crosstalk of approximately 6%.

Furthermore, for conventional 3D displays, the viewing is usually limited at some special viewing positions. Inconvenient feelings hinder our natural vision. From the angular measurement shown in Fig. 6-19, when our left eye is located at viewing angle between -7.5˚ and -20˚ while our right eye at viewing angle between 7.5˚ and 20˚, crosstalk is of less than 10%. In consequence, the position of viewer can be moved within the range of viewing angle between -7.5˚ and -20˚. Therefore, the

viewing distance can be adjusted within 90 and 250 mm. In addition, the viewing angular range demonstrated a steep slope between -7.5˚ and -10˚. In contrast, a more gentle slope was exhibited between -10˚ and -20˚. Out of the viewing angular range, the 3D image perception can not be obtained. As a result, the 3D reception becomes blurred faster when the viewer moves far away the display. In contrast, the 3D reception becomes blurred slower when the viewer moves toward the display. Besides, crosstalk was caused by the reflected rays at the end surface of lightguide. Crosstalk can be further improved by increasing light utilization efficiency. If light is fully utilized, there is no light reflecting, thus, reducing crosstalk. Besides, by reducing the thickness of the grooved lightguide from 1 mm to 0.8 mm, the light utilization efficiency can be further enhanced by 20% because of the increasing opportunities of light hitting on the grooves of the lightguide.

Response time of LC

Based on time-multiplexed approaches, a fast switching LC panel is essential to sequentially obtain images in our left and right eyes. In consequence, response time of LC and the image flicker are main concerns. If the two field sequential images are displayed with the frame frequency faster than 60 Hz, the flicker is undistinguishable by human eyes. In this case, sequentially switching two images, response time of LCD needs to be of less than 8 ms. There are several major approaches to achieve fast response time, for example, ultra-thin twisted nematic (TN) LC with overdriving technology, optical compensated bend (OCB) LC cell, and ferroelectric LC (FLC), etc..

The response time of LC is affected by rising time and decay time. In general, rising and decay times of LC are defined as the duration between 10% and 90% transmittance. In convention, response time of TN LC can achieve less than 25ms.

Eqs. (6-5) and (6-6) illustrate the affecting factors of rising time and decay time.

$$\tau_{rise} = \frac{\gamma_1 d^2 / K\pi^2}{(V/V_{th})^2 - 1} \quad (6\text{-}5)$$

$$\tau_{decay} = \frac{\gamma_1 d^2 / K\pi^2}{|(V_b/V_{th})^2 - 1|} \quad (6\text{-}6)$$

where γ_1/K is the viscosity of LC, d is the cell gap, V and V_b are applied voltage. Therefore, in order to reduce the rising time and the decay time, low viscosity, higher Δn and thinner cell gap LC are essential. In addition, we can utilize overdriving technology to apply a higher voltage.

The optical response waveforms by overdriving/undershooting methods are shown in Fig. 6-20. The fast response driving method enables transition luminescence value to reach the expected luminescence value faster by adding appropriate overdrive voltage or lacking undershooting voltage.[12] By overdriving/undershooting approaches, 90° TN LC panel of ultra thin cell gap (2 μm) and high Δn was fabricated to achieve fast response time. As shown in Fig. 6-21, rising and falling times were measured to be 4.7 ms and 2.4 ms, respectively. Response time, which is the sum of rising and falling times, can reach 7.1 ms.

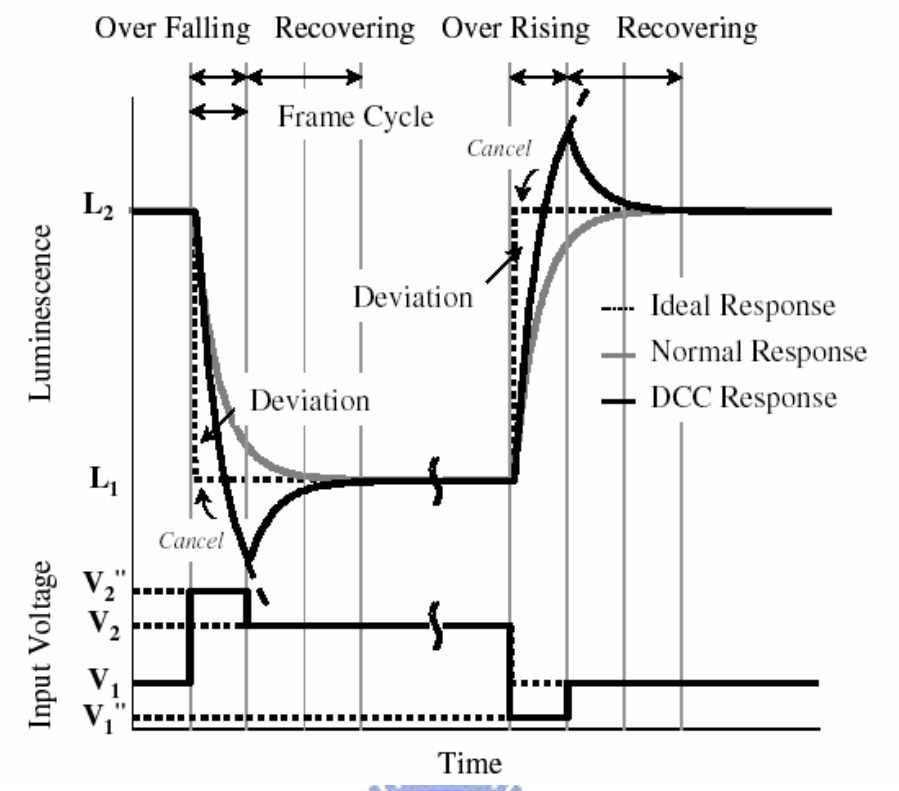

Fig. 6-20. Optical response waveforms by overdriving/undershooting methods.

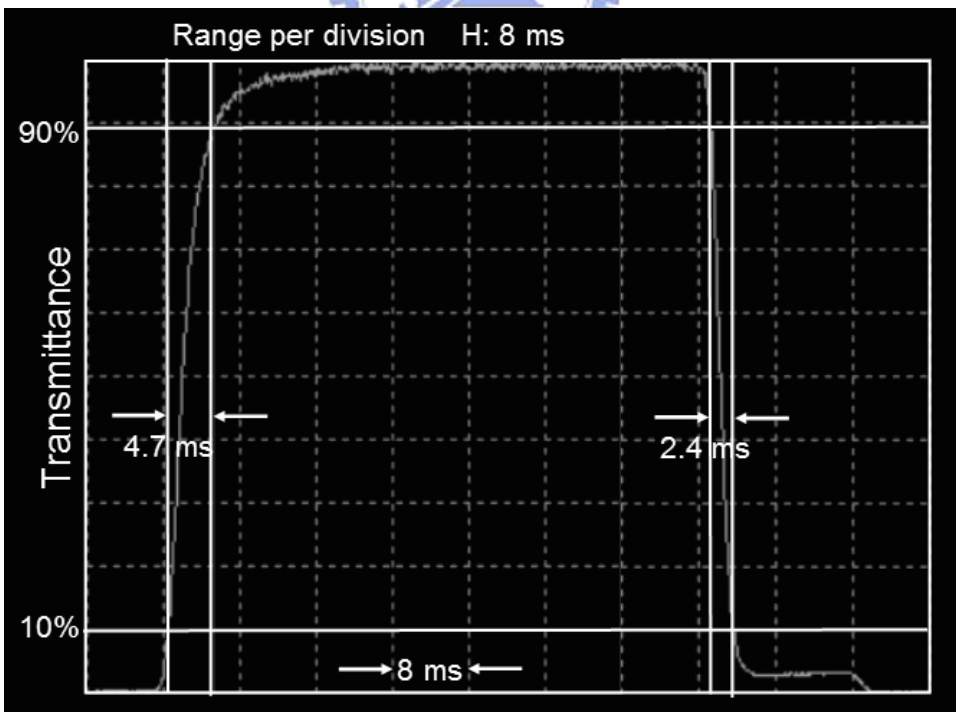

Fig. 6-21. Rising and falling times measured as the duration between 10% and 90% transmittance.

For the second approach, we utilize OCB LC to achieve response time of approximately 5 ms. The optical structure is schematically shown in Fig. 6-22, which is composed of a biaxial film (usually negative birefringence) and a π-cell structure. An exceptionally fast response time is associated with this specific alignment control structure, where the molecular alignment turns by 180 degrees across the cell. If a field is applied, molecules pointing 45 degrees with respect to the field experience the maximum torque so that the rising time is significantly reduced (1 ms or less). When the bias is released, the tilted deformation generates a large reverse torque. At the middle of the cell, the alignment remains vertical. The cell gap can be bisected into two sub cells. Therefore, the falling time is also very short (4 ms). The decay time can be made even shorter by using a backflow effect of LC.[13]

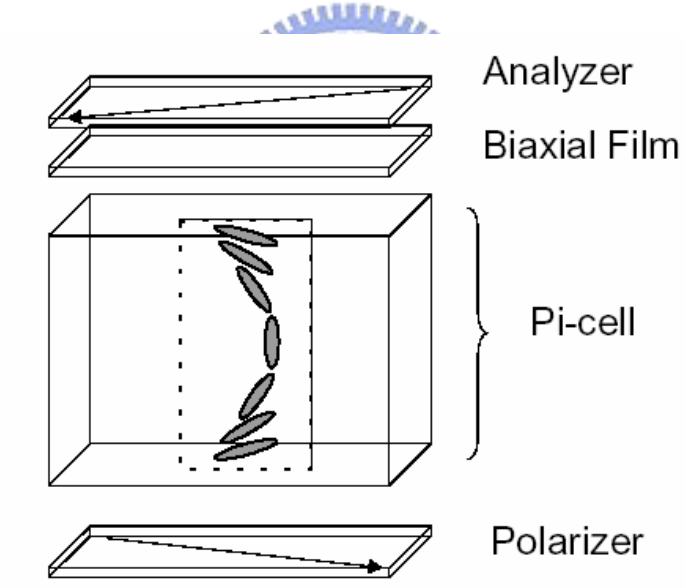

Fig. 6-22. Schematics of optical structure of OCB LC.

For ferroelectric LC, the response time can be as fast as 100~400 μs. However, the applied voltage is usually higher than 30V. Additionally, the fabrication is somehow critical. Imperfection of the LC alignment causes light leakage, thus, degrading the contrast ratio. The above reasons usually constrain its application.

6.7 Impulse Driving

Because the images observed by the respective eyes are slightly shifted due to different viewing angles, we need to input two images for our left and right eyes. Generally, we can utilize camera which is placed at the position of the left and right eyes, i.e. at different viewing angles, to capture two 3D images. Fig. 6-23 demonstrated the images for the left and right eyes, respectively.

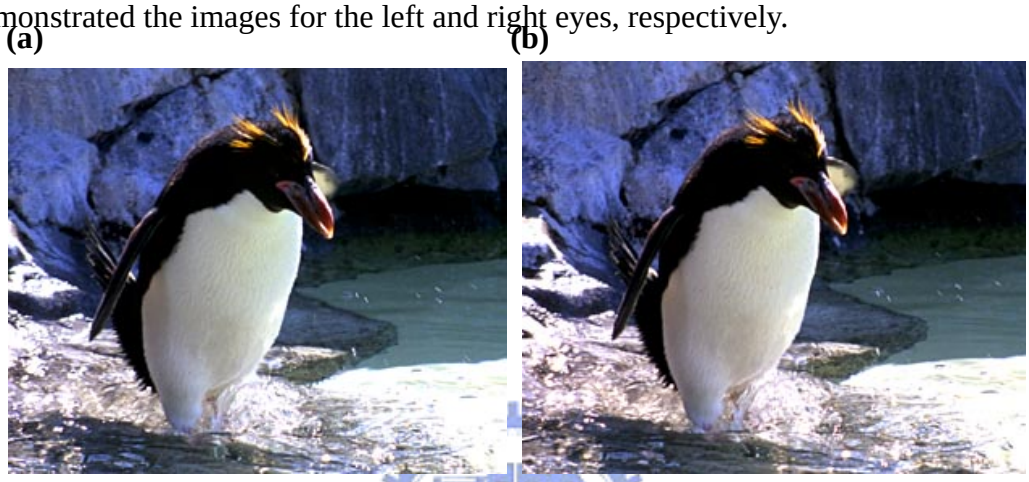

Fig. 6-23. 3D images for (a) left and (b) right eyes.

Two images are sequentially switching on the LC panel. However, crosstalk was caused while refreshing the images of the previous frame. In order to avoid crosstalk while refreshing the images, two main impulse-driving methods, black image data insertion and blinking backlight, are proposed, as shown in Fig. 6-24.[14]

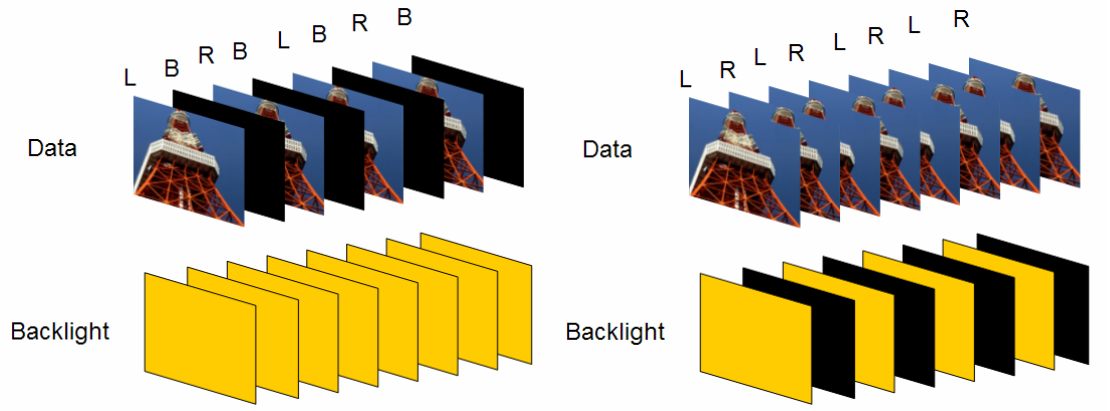

Fig. 6-24. Impulse driving implemented by (a) black image data insertion and (b) blinking blacklight.

In the black image data insertion method, the black image data is inserted sequentially between the left and right eye image data in each frame. However, for this approach, the frame frequency is becoming double. The response time of LC hence needs to become half, i.e. less than 4 ms. It is very difficult for nowadays technologies. Therefore, we adopted the latter approach, which is the so-called blinking backlight, for less demanding on LC response time. The blinking backlight method is implemented by turning off the backlight's LED light sources periodically.

The photographs of a directional backlight with an LCD panel at the positions of left and right eye are demonstrated in Figs. 6-25 (a) and (b), respectively. By switching on light source 1, an image on the LCD is clearly visible at the left eye's position (Fig. 6-25 (a)). At the same time, an image is hardly visible at the right eye's position (Fig. 6-25 (b)).

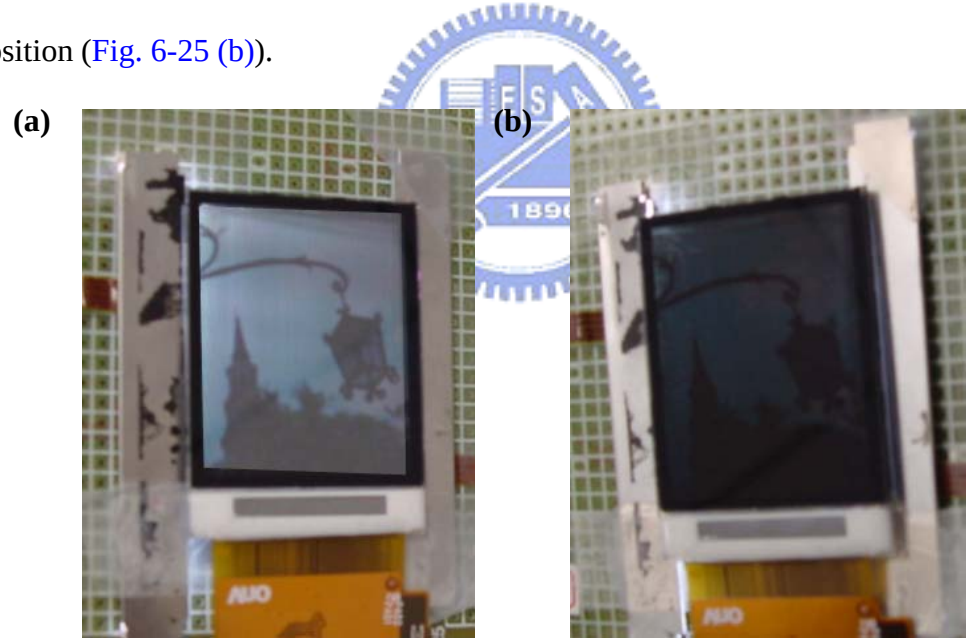

Fig. 6-25. Demonstrated photographs of a directional backlight with an LCD panel at the positions of (a) left and (b) right eye.

The crosstalk is approximately 6%, which is less than the minimum requirement of 10%. Therefore, it is confirmed that the directional backlight can meet the required properties of time-multiplexed 3D displays. Furthermore, 2D/3D compatibility is

provided by switching on two sets of light sources simultaneously or sequentially, respectively. 2D image perception is achieved when there is no binocular disparity while simultaneously observing the same image. In contrast, 3D image perception is obtained by combining sequentially switching images in our brain.

6.8 Conclusion

A fast switching, directional backlight with LC panel was designed and fabricated to realize 3D mobile display. A grooved-lightguide in combination with asymmetric focusing foil was utilized to redirect light to our eyes. The groove structures of the focusing foil with rotation from -1.5° to 1.5° in gradient was designed. Additionally, the pitch ratio of the grooved lightguide to the focusing foil is of less than 3 to suppress the moiré phenomenon. The measured crosstalk of the backlight module with LC panel is of less than 6%. In addition, the blinking backlight was applied on the module to reduce the crosstalk while refreshing the image. The response time of LC can reach 7.1 ms, so that the two field sequential images are displayed without the flicker. The photographs of the directional backlight with an LCD panel are also included to demonstrate the functioning of the devices. By switching on light source 1, an image on the LCD is clearly visible at the left eye's position while hardly visible at the right eye's position. Hence, the directional backlight is confirmed to meet the required properties of time-multiplexed 3D displays. Furthermore, the proposed autostereoscopic display module provides 2D/3D compatibility without degrading display resolution and efficiency in switching mode.

6.9 References

[1] R. Okoshi, Proceeding of IEEE, Vol. 68, p.548 (1980).

[2] P. St-Hilaire, S. A. Benton, M. Lucente, J. D. Sutter, and W. J. Plesniak, Practical

Holography VII: Imaging and Materials, SPIE Proceeding, Vol. 1914, p. 188 (1993)

[3] US Patent No. 5,854,613 (1998)

[4] H. Morishama, H. Nose, N. Taniguchi, K. Inoguchi, S. Matsumura, Society Information Display (SID) Digest, p.923 (1998).

[5] I. Sexton, SPIE Proceedings, Vol. 1083, p.84 (1989).

[6] N. Eiji, H. Goro, Y. Atsuhiro, M. Ken, U.S. Patent 5,831,765 (1996).

[7] B. Jesse, U.S. Patent 6,157,424 (1998).

[8] R. Robert, G. John, A. M. Simon, U.S. Patent application no. 20,020,001,128 (2000).

[9] A. R. L. Travis, S. R. Lang, Proceeding of Society Information Display (SID), Vol. 32, p.279 (1991).

[10] Y. Yeh, and L. Silverstein, Society Information Display (SID) Digest, p.826 (1991).

[11] A. Lit, Am. J. Psychology, Vol. 62, p.159 (1949).

[12] K. Kawabe, T. Furuhashi, Society Information Display (SID) Digest, p.998 (2001).

[13] E. Lueder, *Liquid Crystal Displays*, John Wiley & Sons, p.47 (2000).

[14] K. Allen, Information Display, Vol. 20, No. 6, p.22 (2004)

[15] http://www.research.philips.com/technologies/display/ov_3ddisp.html

[16] S. Jung, J. H. Park, H. Choi, B. Lee, Optics Express, Vol. 11, No. 12, p.1346 (2003)

[17] J. S. Jang, Y. S. Oh, B. Javidi, Optics Express, Vol. 12, No. 4, p.557 (2004)